Seismic performance of PCa beams with mechanical joints at beam-ends.

Satoshi Kake

Takenaka Corporation, Japan.

Yuji Ishikawa, Takashi Doi, Motonobu Maekawa

Takenaka Corporation, Japan.

ABSTRACT: This paper presents the results of an experimental study on the seismic performance of precast reinforced concrete deep beams using mechanical joints at beam-ends. Lateral loading tests are carried out to investigate the flexural and shear performance of these beams, where the experimental parameter is the failure mode (flexural failure and shear failure). The specimen, which was intended to have a flexural failure, experienced tensile yielding of the beam longitudinal bars near the mechanical joints. The specimen, which was intended to have a shear failure, experienced a shear diagonal tension where neither yielding at the mechanical joints nor fracture were observed until the end of the experiment. As to the ultimate strength of the specimens, while the ultimate flexural strength was estimated using the formula in AIJ (Architectural Institute of Japan) standard, the ultimate shear strength was estimated using the empirical equation of Arakawa. By the influence of the tension shift, the critical section of the specimen, which was intended to experience a flexural failure, was located 0.6D (D: beam depth) away from the beam end. Therefore the flexural ultimate strength was estimated using the flexural strength formula that considers internal forces at the critical section of the beam.

1 INTRODUCTION

In recent years, structural construction methods using precast members for reinforced concrete buildings in Japan have become various and their number increased, because high quality buildings and high productivity are desired and lack of skilled construction workers. Generally, the connection of precast beams is often set at their mid-spans because stresses are relatively small. However, there are cases in which these connections are set at beam ends using mechanical joints because of some restrictions related to the design and construction of buildings (Fig.1). Furthermore, because building owners request wide interiors and high-seismic safety, the need for base-isolated buildings has increased. Based on such conditions, designers, generally, adopt spandrel beams. In this paper, the seismic performance of a precast spandrel beam using mechanical joints at its ends was examined by a static loading test.

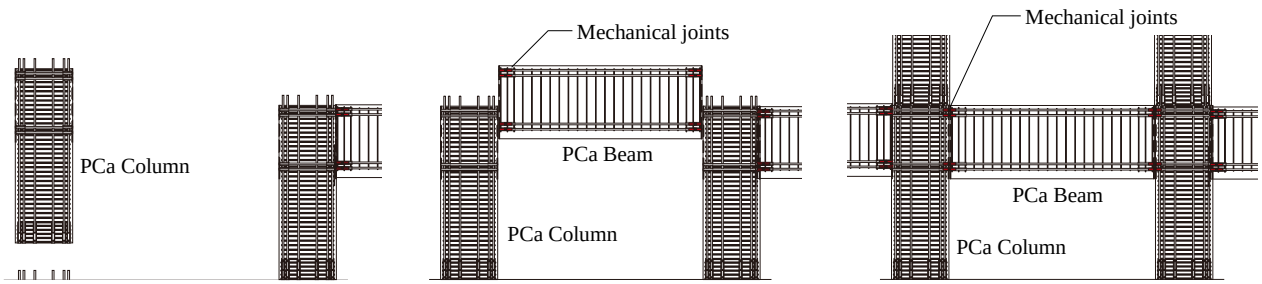

Step-1: Setting precast columns

Step-2: Setting precast beam

Step-3: Completing beam-ends connection

Fig.1 Outline of construction stages

2 OUTLINE OF EXPERIMENTAL RESEARCH

2.1 Specimens

The design parameters of the beam specimens and their corresponding values are given in Table 1. The details of the specimens are given in Fig.2. The specimens are cantilevers scaled to 2/3 of the actual size, with mechanical joints located at the cantilever's embedment. To insure ductile structural behaviour of such jointed beams and investigate their shear property, two specimens are constructed. The chosen experimental parameter is the failure mode (flexural failure and shear failure). Based on the weak-beam strong-column concept, the specimen KB-F is representative of such beams that are part of RC buildings in which hinges form at beam-ends. To prevent the occurrence of any abrupt failures in such beams, the specimen KB-S is also investigated. The failure mode is adjusted by a combination of steel strength and amount of the longitudinal bars and stirrups. The section's aspect of the specimen is rectangular B×D=220mm×1060mm (D/B=4.82), and its length is 1950mm (shear span ratio: M/Qd=2.08). The specimens were produced by the indicated procedure shown in Fig.3. After adjusting the position of the beam-cantilevers, the longitudinal bars of the beams were spliced to the longitudinal bars of the stub by the mechanical joints that were provided within the beams by sliding them partly into the stub. Finally, high-strength cement paste was, first, filled into the mechanical joints, and when the cement paste hardened, grout was filled into the sheaths and gap-joints.

Table1 Description of test specimens

Specimen	KB-S	KB-F
Assumed failure mode	Shear failure	Flexural failure
Concrete strength:f'_c , (Elastic modulus:E_c)	55.5MPa , (3.07×10^4MPa)	
Section (B×D)	220mm×1060mm	
Length:L (shear span ratio:M/Qd)	1950mm (M/Qd=2.08)	
Longitudinal Bars (Grade) , [p_t]	6-D19(SD980)*1 , [0.84%]	6-D19(SD390)*2 , [0.84%]
Stirrups (Grade) , [p_w]	2-D6@100(SD295A)*3 , [0.29%]	2-D6@75(SD785)*4 , [0.38%]
Q_{su}(shear strength) /Q_{mu}(flexural strength)*5	0.61	2.02

Notation p_t : tensile reinforcement ratio, p_w : shear reinforcement ratio

* SD□□□, SD : Steel Deformed , □□□ : Specified yield strength
Steel bars Cross-sectional Area D19:287mm^2, D6:32mm^2

*1 Yield strength fy=1149MPa , Modulus of elasticity Es=1.95×10^5MPa

*2 Yield strength fy=452MPa , Modulus of elasticity Es=1.94×10^5MPa

*3 Yield strength fy=379MPa , Modulus of elasticity Es=1.83×10^5MPa

*4 Yield strength fy=898MPa , Modulus of elasticity Es=1.89×10^5MPa

*5 Design results of shear and flexural strength by AIJ Guideline 2010

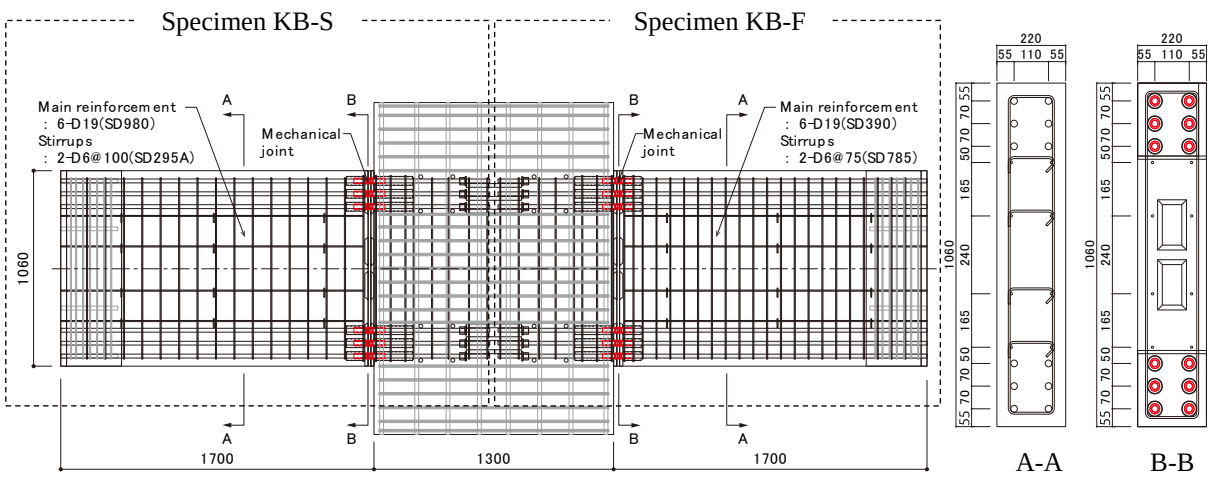

(a) Elevation (b) Section

Fig.2 Geometry and detailing of specimens

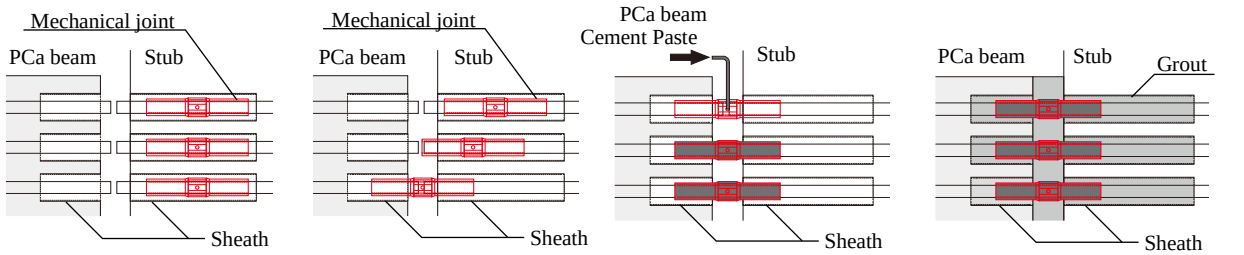

Step-1: Setting precast beam

Step-2: Sliding mechanical joints

Step-3: Cement paste filling into joints

Step-4: Grout filling into sheaths and gap

Fig.3 Beam ends' connection stages

2.2 Material characteristics

The compressive strength of concrete is f'_c=55.5MPa. The longitudinal bars of specimen KB-S are of high strength type (SD980) and stirrups are of normal strength type (SD295A). The longitudinal bars of specimen KB-F are of normal strength type (SD390) and stirrups are of high strength type (SD785). As to the cement paste in the mechanical joints and the grout in the gaps, the compression strength is higher than the specimen's concrete strength. The mechanical joints are of screw type made of ductile steel, which the standard yield strength insured by the fabricator is higher than 900MPa.

2.3 Loading procedure

The loading setup is shown in Fig.4. The specimen's stub was fixed at a rigid base by prestressing steel bars. The load was applied vertically at the tips of each cantilever-beams using an oil jack. The loading course, shown in Fig.5, is similar for both specimens. The specimens were subjected to a displacement control mode with increasing cycle amplitudes, represented in terms of the drift angles: R=1, 2, 3.3, 5, (2), 7.5, 10, (5), 15, 20, (5), 30, 40x10^{-3}rad and 50 x10^{-3}rad.
Short amplitudes indicated by numbers in parenthesis were inserted in the loading protocol to simulate actual earthquake loading waves. For each amplitude, the load cycle was repeated twice. The second cycle was used to evaluate the equivalent viscous damping factor.

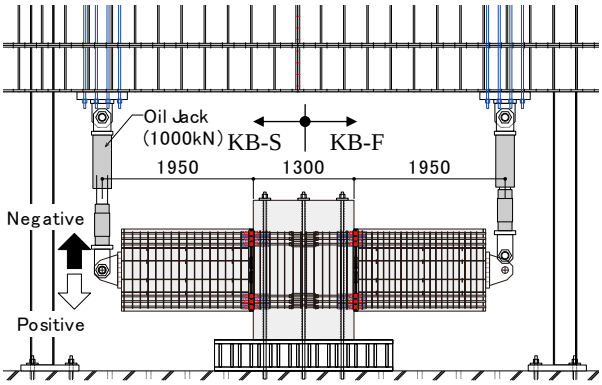

Fig.4 Loading setup

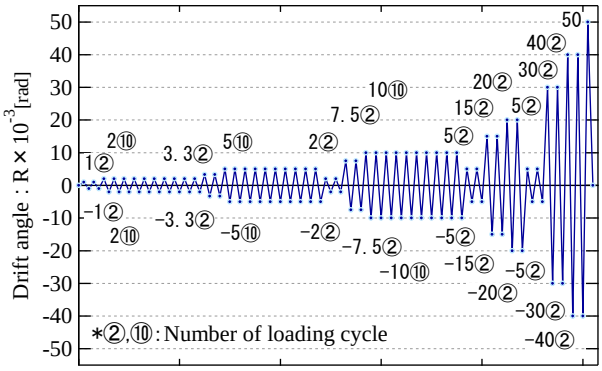

Fig.5 Loading course

3 TEST RESULTS

3.1 Crack progression and Hysteresis loop

The crack patterns of specimens KB-S and KB-F are shown in Fig.6. Fig.7 shows the relationships of the shear force as well as the equivalent viscous damping factor (h_{eq}) to the drift angle. The level at which flexural and shear cracks occurred, and tensile yield point of longitudinal bars and stirrups was reached, as well as the calculation values of the ultimate flexural and shear strengths are also shown in Fig.7. For the specimen KB-F (flexural failure type), flexural cracks appeared, first, near the location of the mechanical joints at the drift angle R=1×10^{-3}rad, then followed by shear cracks by the drift angle R=5×10^{-3}rad. These cracks increased in length and width when load increased. Before the drift angle R=7.5×10^{-3}rad, the tensile yielding of the longitudinal reinforcement layers 1～3 near the

mechanical joints was reached. Finally, flexural cracks occurred at the location 0.6D (D: beam depth) away from the beam's embedment section, the developed flexural shear cracks of the positive and negative loading directions interconnected near the beam's embedment zone, and sliding shear failure was observed. The hinge region is observed within the concrete failure zone of a length 0.6D. This result is larger than the result given in the study of Ohkubo et al. which is 0.1D. Similar events as in specimen KB-F were observed on the specimen KB-S (shear failure type) by the drift angle $R=5\times10^{-3}$rad. After that, before the drift angle $R=15\times10^{-3}$rad, diagonal tension failure occurred, shear strength suddenly decreased and at that time, the test was ended.

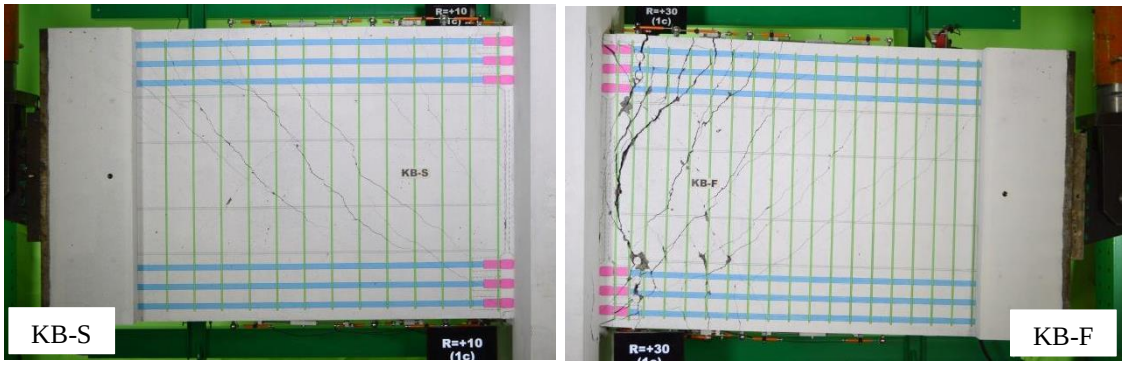

(1) At maximum strength

(2) At end of loading

Fig.6 Crack patterns and failure of beams

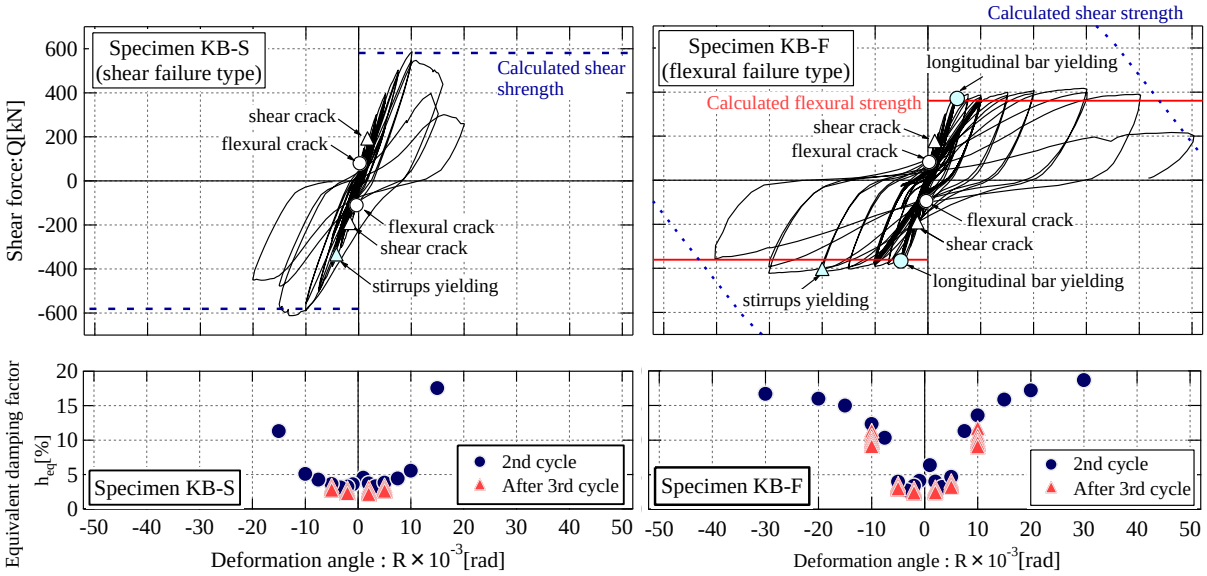

Fig.7 Shear force-deformation angle response and major events

3.2 Elastic Stiffness

Fig.8 shows the relationships of the shear force to the drift angle for both specimens. The calculation and experimental values of the elastic stiffness of each specimen are shown in Table 2. The calculated stiffness value ($k_{e,cal}$) given by formula (3.1), is for ordinary non-precast beams and without mechanical joints at beam-ends

$$\frac{1}{k_{e,cal}} = \frac{1}{k_m} + \frac{1}{k_s} \qquad k_m = \frac{3E_c I_e}{L^3}, k_s = \frac{GA}{\kappa L} \qquad (3.1)$$

where $k_{e,cal}$: elastic stiffness, k_m: flexural stiffness, k_s: shear stiffness, E_c : concrete elastic modulus, I_e: second moment of inertia, considering reinforcement, L: member length, G: elastic shear modulus, A: section area and κ:form factor. The experimental elastic stiffness was measured for each specimen at the drift angle R=0.1×10^{-3}rad. the ratio of the experimental value to the calculation value was in the range 0.90～0.98. The formula (3.1) estimated precisely the elastic stiffness of the specimen.

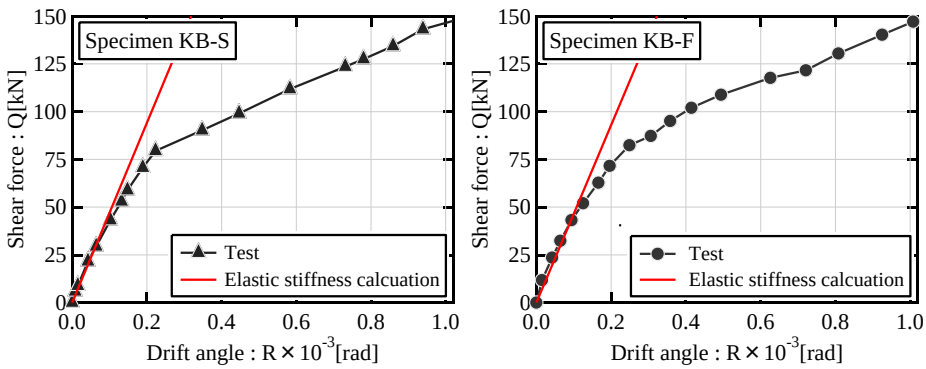

Fig.8 Envelope curve and elastic stiffness

Table2 Elastic stiffness (calculation and experimental values)

Specimen	Experiment value $k_{e,exp}$[kN/mm]	Calculation value $k_{e,cal}$[kN/mm]	$\frac{k_{e,exp}}{k_{e,cal}}$
KB-S	319.6	356.3	0.90
KB-F	345.2	352.2	0.98

3.3 Tensile stress of Mechanical joint

The tensile stress variation of one outside mechanical joint was measured for each specimen using strain gauges. The stress variation is shown in Fig.9. For both specimens, tensile yielding and rupture of joints were not observed during the test. For the specimen KB-F (flexural failure type), the stress of the mechanical joint had kept increasing until the tensile yielding of longitudinal bars was reached, then the stress level was unchanged, although loading increased. For the specimen KB-S (shear failure type), the stress of the mechanical joint increased as the drift angle had become large. When the diagonal tension failure occurred at drift angle R=15×10^{-3}rad, the stress decreased.

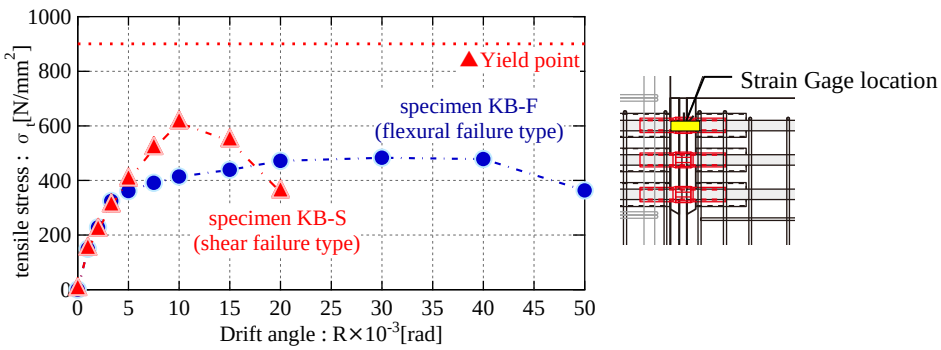

Fig.9 Tensile stress variation of outside mechanical joint

3.4 **Deformation distribution**

To measure the deformations of the specimens, displacement transducers were installed as shown in Fig.10. The deformations of the specimens consisted of the flexural, shear and slip deformations. The flexural deformation of each specimen was measured by the axial displacement transducers. The slip deformation was measured by the vertical displacement transducer that was set at the beam-end (Fig.10). The shear deformation of each specimen was obtained by deducting the measured flexural and slip deformations from the total measured deformation. The deformation distribution of each specimen is shown in Fig.11. For the specimen KB-F (flexural failure type), the observations showed that the shear deformation increased with shear cracks. The flexural and slip deformations increased after tensile yielding of longitudinal bars was reached. Finally, the slip deformation at the beam-end gradually increased, and the specimen shifted to sliding shear failure. For the specimen KB-S (shear failure type), it was noticed that the shear deformation increased with the development of shear crack, while the slip deformation was unchanged.

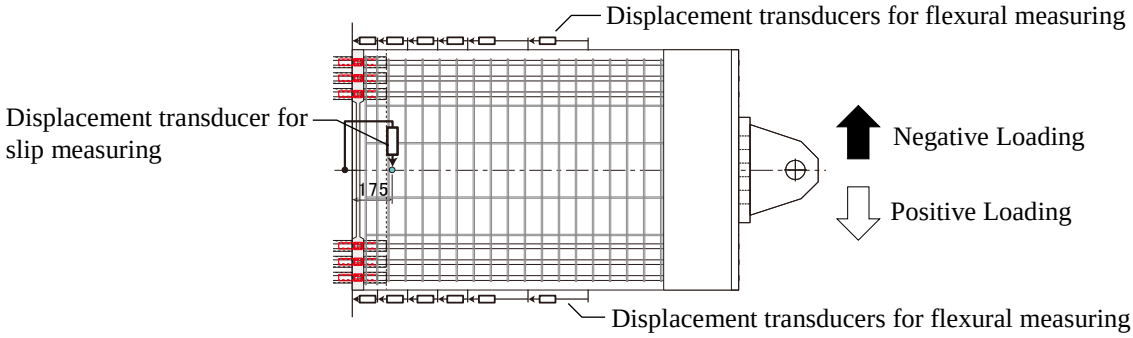

Fig.10 Displacement transducer setup

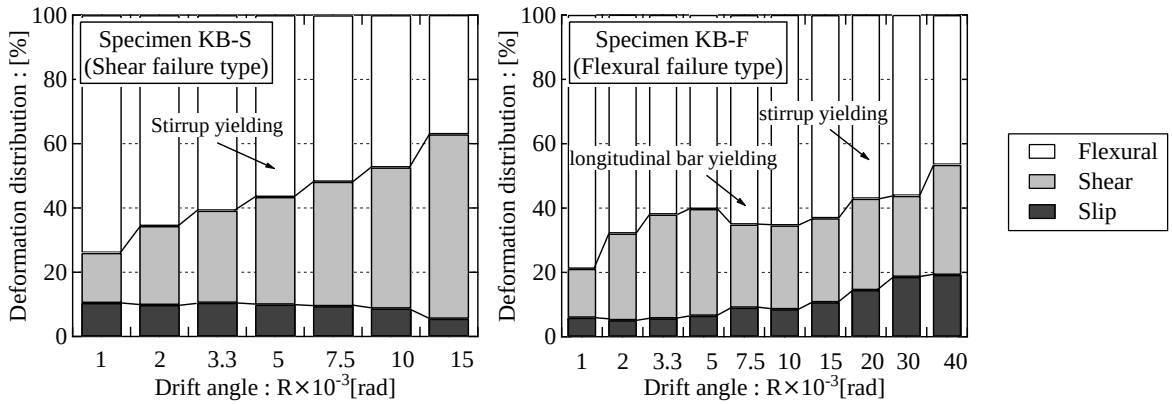

Fig.11 Deformation distribution

4 **EVALUATION OF ULTIMATE STRENGTH**

The crack pattern of specimen KB-F when it reached its ultimate strength is shown in Fig.13. The stress distributions of a longitudinal bar and a stirrup of the specimens at their ultimate strengths are shown in Fig.12. For specimen KB-F(flexural failure type), when the ultimate strength was reached, large flexural cracks occurred at the location 0.6D away from the embedment section, tensile yielding of the three longitudinal reinforcement layers at the location 0.75D occurred, and the stirrups at the location 0.45D experienced tensile yielding. For specimen KB-S (shear failure type), when the ultimate strength was reached, the longitudinal reinforcement had not yielding, but the stirrups at the mid of the cantilever-beam experienced tensile yielding. The ultimate strength of each specimen is evaluated from the stress state and crack pattern.

4.1 **Flexural failure type**

The flexural ultimate strength of the specimen KB-F was calculated by AIJ standard formula (4.1).

$$Q_{mu1} = M_u / L$$
$$M_u = 0.9 a_t \cdot \sigma_y \cdot d \qquad (4.1)$$

where, Q_{mu1} : flexural ultimate strength, L : length, a_t : amount of longitudinal bar on tensile side, σ_y : yield stress, d : effective depth. The calculation and experimental value of flexural ultimate strength of specimen KB-F are shown in Table4. The ratio of the experimental value to the calculation value was in the range 1.15～1.17. The AIJ standard's formula estimated precisely the ultimate strength of the specimen considering three-layer reinforcing. To evaluate the flexural ultimate strength relative to spandrel beams, the proposed formula of Paulay et al. was used considering an assumed shear crack (Fig.14 and formula (4.2)).

$$M_1 = z_b T_2 + 0.5 z_b V_s \qquad (4.2)$$

where, M_1 : moment at section 1, z_b : the internal lever arm, T_2 : flexural tension force at section 2, V_s : vertical tension generated in stirrups. The ratio of the experiment value to the calculation value based on the proposal of Paulay was in the range 0.89～0.90, indicating an unsafe margin. This result shows that the calculation value was excessively estimated because of an inaccurate location of the critical section, which is z_b (=0.8D), and the effective strength of the stirrups wasn't considered. Therefore, by assuming the maximum strength of the specimen KB-F as the flexural ultimate strength and substituting it into the formula of Paulay, the actual location of the critical section was calculated. The calculated value of the critical section of specimen KB-F is shown Table3.

Table3 The location of critical section

Positive Loading	Negative Loading	Average
657mm(0.62D)	700mm(0.66D)	679mm(0.64D)

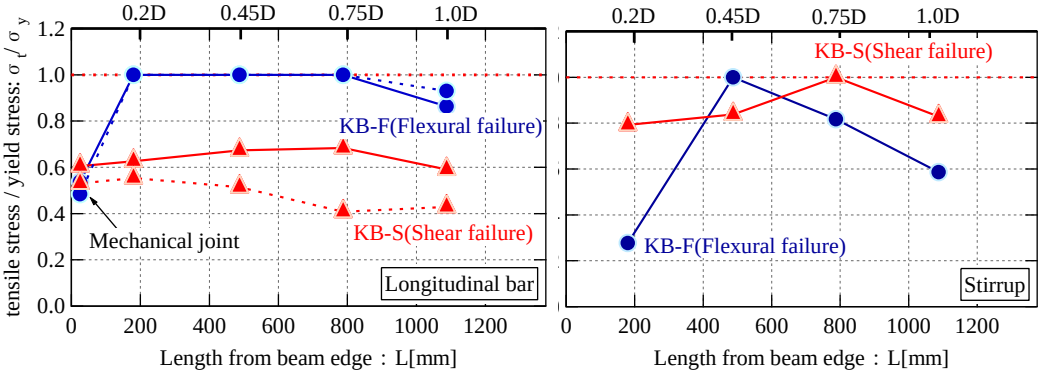

Fig.12 Stress distributions at maximum strength

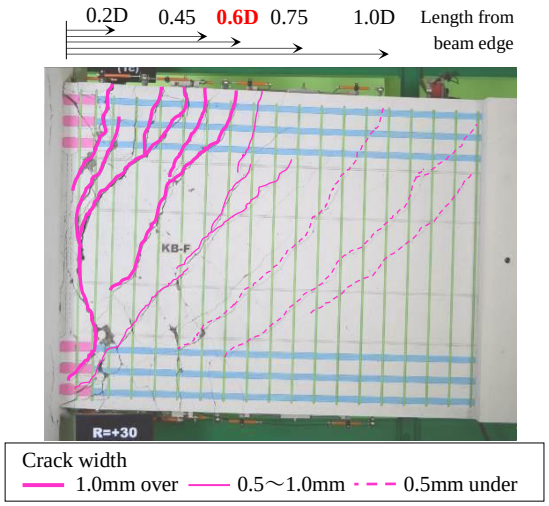

Fig.13 Crack pattern at maximum strength

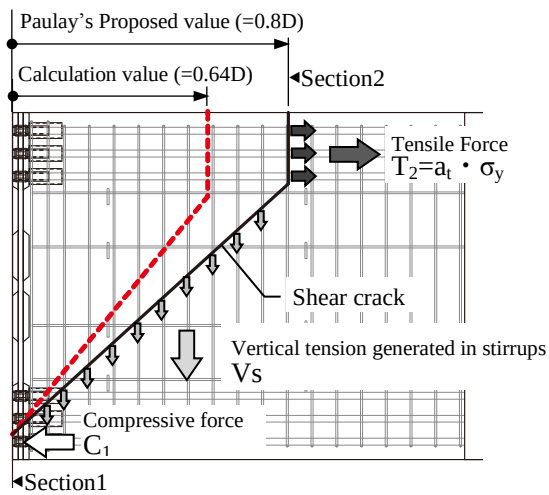

Fig.14 Failure mechanism

The critical of section is found to be at 0.62D (positive loading) and 0.66D (negative loading), and the average value of the positive and negative loadings is 0.64D. Similar results were observed at the crack state (Fig.13). Because the mechanical joints are set by the location 0.1D and the hinge zone is set by the location 0.5D, and their summation gives the location of the critical section near to 0.6D.

4.2 Shear failure type

As shown in Fig.11, the stress of stirrups at the ultimate strength reached yield level at the mid of the cantilever-beam when diagonal tension failure occurred. The shear ultimate strength was calculated by Arakawa's mean formula (4.3).

$$Q_{su} = \left(\frac{0.068 k_u k_p (18+\sigma_B)}{M/Qd + 0.12} + 0.85\sqrt{p_w \cdot {}_w\sigma_y}\right) bj \qquad (4.3)$$

where, k_u: form factor, k_p=0.82$p_t^{0.23}$, p_t :main reinforcement ratio[%], σ_B: compressive strength, *M/Qd*: shear span ratio, p_w: shear reinforcement ratio, σ_y:yield stress, *b*: width, *j*: internal lever arm. The calculation and experimental values of the shear ultimate strength of specimen KB-S are shown in Table4. The ratio of the experimental value to the calculation value was 1.04～1.09. Arakawa's mean formula estimated precisely the ultimate strength of the specimen with enough safety margins.

Table4 Shear ultimate strength (calculation and experimental values)

formula	specimen type	Calculation value Q_{cal}[kN]	Experimental value Q_{exp}[kN]	Q_{exp} / Q_{cal}
AIJ Standard formula	Flexural	360.9	416.8(-422.7*)	1.15(1.17*)
Paulay's formula		470.3		0.89(0.90*)
Arakawa's mean formula	Shear	562.4	586.5(-612.0*)	1.04(1.09*)

* Negative loading

5 CONCLUSIONS

This paper presents the results of an experimental study on the seismic performance of precast reinforced concrete spandrel beams using mechanical joints at beam-ends. The following conclusions can be drawn.

1) For shear failure type and flexural failure type specimens, tensile yielding and rupture of mechanical joints were not observed during the test. The tensile yielding of the longitudinal bars near the mechanical joints was reached.

2) The ultimate strength of precast reinforced concrete spandrel beams using mechanical joints at beam-ends was estimated precisely and with safe margin by AIJ (Architectural Institute of Japan) standard formula and Arakawa's mean formula.

3) The calculated location of the critical tensile section of flexural failure type specimen was at 0.6D away from the embedment section. Similar result was observed at the crack state.

REFERENCES:

Y.Ishikawa, H.Kimura, M.Miyuchi, A.Sumi and H.Ueda. 2004. Study on Structural Behavior of R/C Beams using Lap Splices of Headed Longitudinal Bars. *Conrete research and techonology*. 15(2). 1-11.

T/Paulay and M.J.N.Priestley. 1992. SEISMIC DESIGN of REINFORCED CONCRETE and MASONRY BUILDINGS

M.Ohkubo, S.Shioya and T.Ano. 1989. Inelastic Behavior of Reinforced Concrete Spandrel-Beams. *Proceedings of the Japan Concrete Institute*. 11(2). 63-68.

AIJ. 2010.Standard for Structural Calculation of Reinforced Concrete Structures.*Architectural Institute of Japan.*

AIJ. 1999. Guidelines for Earthquake Resistant Reinforced Concrete Buildings Based on Inelastic Displacement Concept.*Architectural Institute of Japan.*